Measurements on a Thermal Gradient Gas Lens

WILLIAM H. STEIER, MEMBER, IEEE

Abstract—If a cool gas is gently blown through a hot tube, the temperature distribution within the tube is such to make a positive optical lens which has no surfaces for scattering and reflection. These thermal gas lenses are of interest for long-distance optical transmission. In this paper the temperature distributions inside the tube and the optical properties of these lenses have been studied in detail.

The temperature distributions inside a 0.250-inch ID heated tube were measured with a small thermocouple probe. The results agree with theory except for the gravity effect which displaces the coldest point below the center of the tube.

The optical properties of a 0.250-inch ID 17.8-cm long lens were measured with interferometers at 6328Å. The temperature profiles, paraxial focal distances, and aberration coefficients have been measured under a variety of experimental conditions.

I. Introduction

THERMAL GAS LENSES for guiding light beams were considered previously by several authors [1]–[3], and their possible value in long-distance optical transmission was indicated. The gas lens used in this work consisted of a heated metal tube through which a cold gas was gently blown. The resultant temperature distribution and, hence, density variations of the gas within the tube is such to make a positive optical lens. This lens has been analyzed by Marcuse and Miller [2] and later in more detail by Marcuse [3]. Some preliminary experimental measurements have been reported by Beck [4].

This paper reports a detailed experimental investigation of this lens under a variety of conditions. The temperature profiles within the tube were measured and compared to the theory. The optical properties of the lens were measured by interference techniques. The focal distance and aberrations of the lens were measured and where possible they were compared to the theory.

II. Temperature Measurements

As the first step in investigating the gas lens, the temperature profiles of the gas in the tube were measured. The theory of the temperature distribution assumed by a cool gas blown through a hot tube of constant temperature has been considered by Jakob [5] and Marcuse and Miller [2]. The theoretical temperature profiles can be calculated from formulas given in these references.

The experimental arrangement for measuring the temperature profiles is shown in Fig. 1. The tube was 0.250-inch ID brass. A small movable thermocouple probe was inserted axially in the gas exit end of the heated tube. To minimize the end effects, the probe was inserted 0.50 inch in from the end of the hot tube. This was as far as was practical because of the fragile probe. The thermocouple probe was then moved radially by a micropositioner and the temperature profiles were measured.

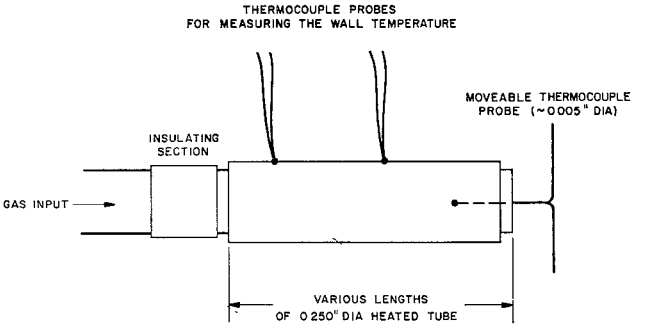

Fig. 1. Experimental arrangements for measuring temperature profiles inside the heated tube.

The length of heated tube was varied to give the effect of measuring the temperature at various points down a long heated tube. The tube was heated electrically. The flow system consisted of pressure regulators and a stabilizing tank to insure a constant volume flow.

Typical measured temperature profiles are shown in Figs. 2 and 3. The distance z is measured from the gas input end of the hot tube to the plane of measurement. The effect of gravity can be clearly seen in the vertical profiles of Fig. 2. Gravity causes the coldest spot in the tube to be below the tube center. Figure 3 was measured in the horizontal plane and is symmetrical about the center.

Also shown on the vertical profile as dashed curves are the theoretical profiles. The theoretical curves have been shifted downward in the tube so their coldest point falls at the same radial position as the measured coldest point.

Generally, it can be said that the measured profiles agree with the theory except for the convection effect. Convection displaces the coldest point below the tube center. The temperature gradients in the upper part of the tube are less than predicted, and in the lower part of the tube are greater than predicted. The temperature profiles were also checked using N_2 gas, lower wall temperatures, and higher flow rates. The same agreement was found there. As expected, it was found that the convection effect is larger in CO_2 than in N_2.

The magnitude of the convection effect and its variation with T_w and gas flow rate can be seen from Fig. 4.

Manuscript received May 5, 1965; revised July 12, 1965.
The author is with Bell Telephone Laboratories, Inc., Holmdel, N. J.

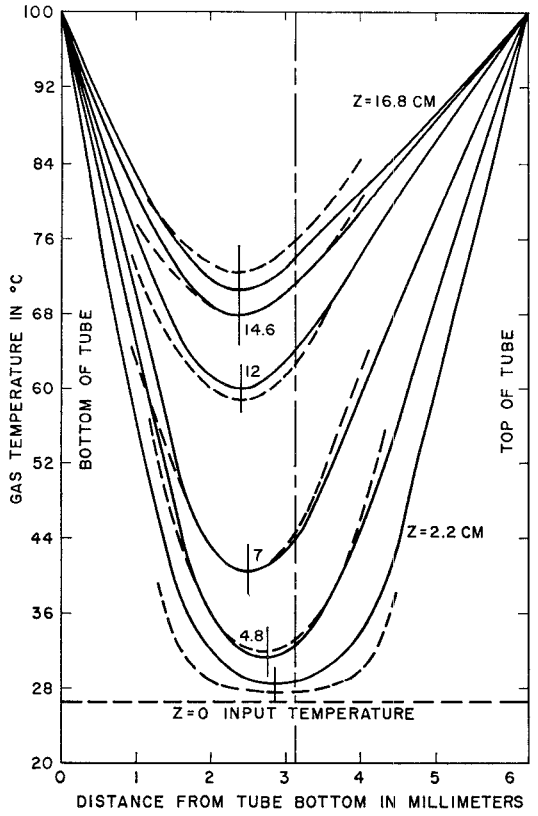

Fig. 2. Vertical temperature profiles for CO_2, $T_w = 100°C$, 1.0 liter per minute gas flow. Dashed curve is theoretical.

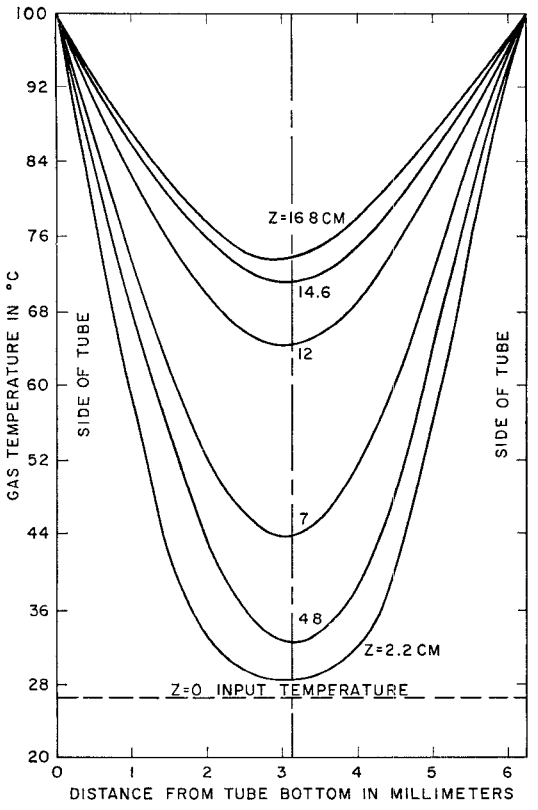

Fig. 3. Horizontal temperature profiles for CO_2, $T_w = 100°C$, 1.0 liter per minute gas flow.

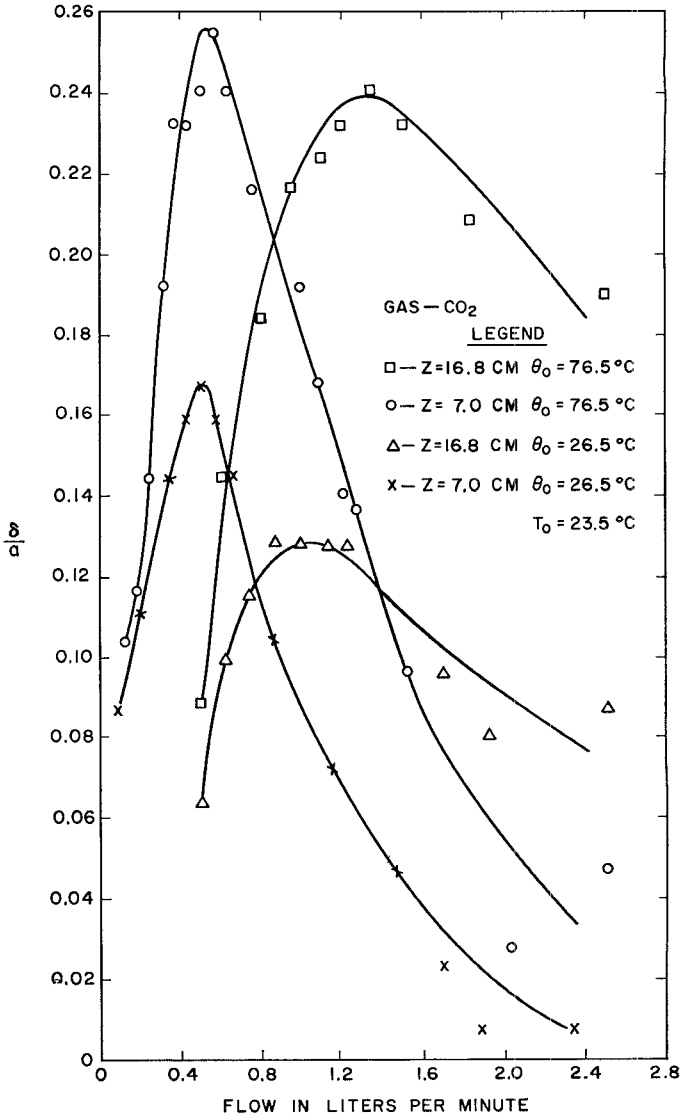

Fig. 4 Gravity effect vs. flow rate. $T_w = 100°C$.

Here the distance δ that the minimum temperature is displaced below the tube axis normalized to the tube radius a is plotted vs. gas flow rate. The points are experimental and the curves are an attempt to fit a smooth curve to the points.

In the figures:

$\theta_0 = T_w - T_0$

T_0 = Gas input temperature

T_w = Wall temperature.

The convection effect is low at very low flows because there is little temperature difference between the gas and the wall after only a short distance down the tube. At high flow rates the convection again decreases, because the gas spends less time in the tube. As expected, the convection is greater for heavier gases and for greater initial temperature difference.

In summary, the theory for the temperature distributions inside the tube seems good except for convection which is not included in the theory.

III. Optical Measurements

The second step in the investigation of the lens was the measurement of its optical properties. It is important, however, to consider first what parameters describe the lens.

A. Description of the Lens

Marcuse [3] showed that the gas lens should have an aberration symmetric about the center of lens. He showed that the focal length and the position of the principal plane vary with radial position in the tube. It is known from the temperature measurements that gravity will cause the lens center to be slightly below the tube center and will cause an asymmetric aberration in the vertical plane.

With interferometric techniques we can measure the shape of a phase front at any point in space. If this phase front comes from a gas lens excited by a plane wave, the properties of the gas lens can be inferred from the shape of the wavefront. To do this we must transform this wavefront back to an equivalent lens at the gas lens position. We cannot tell the position of the principal plane and cannot distinguish between aberrations caused by variation in focal length and aberrations caused by variations in the principal plane position.

We have chosen to relate all measurements to an equivalent lens located at the gas exit end of the heated tube. Since the focal length of a lens should be properly measured from the principal plane we have chosen to call the distance from the exit end of the tube to the point where the ray crosses the axis, the focal distance. We are therefore measuring focal distances in this paper.

We have also chosen to relate all observed aberrations to variations in the focal distance with radial position. These are also measured from the exit end of the heated tube.

From the results of Marcuse [3] and from the temperature measurements, it is reasonable to assume that the gas lens can be described in a vertical cross section by

$$f = f_0(1 + \alpha x - \beta x^2)$$

and in a horizontal cross section by

$$f = f_0(1 - \beta x^2),$$

where

f = focal distance = distance from the end of the hot tube to the point where the ray crosses the axis,
f_0 = focal distance at the center of the lens,
α = parameter describing the gravity aberration,
β = parameter describing the symmetric aberration,
x = distance from the center of the lens.

For some cases the center of the lens was found to be displaced below the center of the tube a sufficient distance Δ to be measured. This displacement is also caused by gravity. The radial distance x is measured from the center of the lens and not the center of the tube. This distance Δ is related to but should not be confused with δ which is the distance the minimum temperature is displaced below tube center.

In relating the observed wavefronts back to an equivalent lens it is assumed that the three-dimensional problem can be handled by two orthogonal two-dimensional problems. Geometrical optics is assumed and the wave propagation is analyzed in two-dimensional cross sections only.

B. Description of the Experimental Lens

The lens used in the experiments is shown in Fig. 5. The heated section was 7 inches long. To assure a laminar flow the gas was introduced through a porous stainless-steel tube and an unheated 8-inch length of tubing was placed before the heated section. The tubes were all 0.25-inch ID brass with their axes horizontal during the measurements.

Brewster angle windows were used on each end. At the exit end the gas was blown out of the tube through several holes placed radially in the tube near the Brewster window. If the heated gas is blown directly out the end of the tube it will cause fluctuations in the light beam as the gas rises. In some cases it was possible to remove the exit Brewster window to see if forcing the gas to flow through the radial holes had any effect on the lens. No measurable effect could be found.

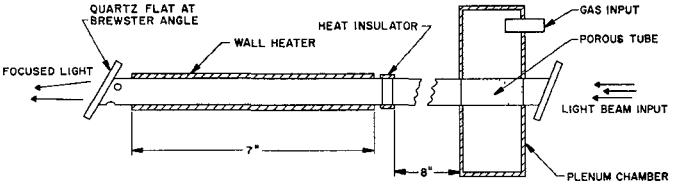

Fig. 5. Experimental gas lens.

C. Interferometer Measurements

The measurement of the three parameters f_0, α, and β is difficult because of the small lens aperture and, hence, limited number of interferences which could be seen. By making the measurements with two different kinds of interferometers, however, it was found the accuracy could be improved. For this reason both a lateral shear interferometer and a Mach-Zehnder interferometer were used.

The lateral shear interferometer was found to give a good first approximation to f_0 even when the aberrations were neglected. The aberration correction to this first approximation was seldom greater than 10 percent. This value of f_0 could then be used in analyzing the Mach-Zehnder ring patterns to obtain the first approximations to α and β.

If was found that the Mach-Zehnder ring patterns are much easier to analyze and give greater accuracy in

finding α and β. The distortions are also easier to visualize from the ring patterns.

A second approximation to f_0 can then be made by using the first approximation of β to recompute f_0 from the lateral shear interferograms. Similarly, a second approximation to β and α can be made from the Mach-Zehnder patterns. In most cases it was only necessary to calculate the second approximations.

1) *Lateral Shear Interferometer Measurements of f_0:* For measuring f_0, the focal distance at the center of the lens, a lateral shear interferometer shown in Fig. 6 was used. The interference pattern where the phase fronts overlap is a series of lines. A photograph of a typical interference pattern is shown in Fig. 7. The crowding of the lines near the bottom is due to gravity. A collimated dominant transverse-mode laser beam at 6328Å of about 5-mm diameter was used as a light source.

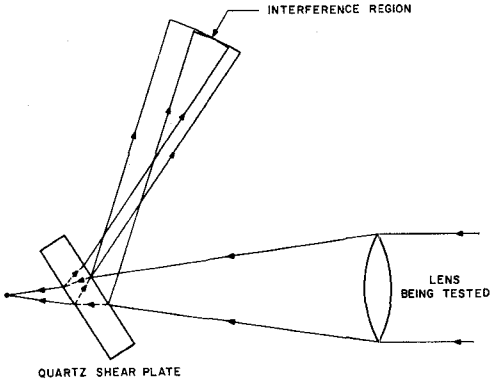

Fig. 6. Lateral shear plate interferometer.

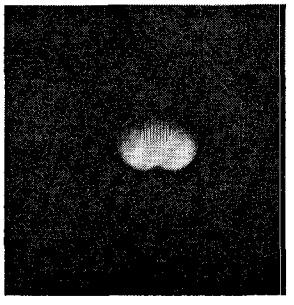

Fig. 7. Typical lateral shear interferogram. CO_2, $\theta_0 = 26.5°$, 1.0 liter per minute.

In Appendix B it is shown that for a horizontally sheared wavefront

$$f_0 = D - \frac{\delta x_0 s}{\lambda}\left[1 - \beta \frac{f_0^3}{(f_0 + D)^3}\frac{s^2}{4}\right],$$

where

s = amount of lateral shear,
δx_0 = spacing of the interference lines in the center of the pattern,
λ = optical wavelength,
D = distance from the point of measurement to the lens position.

The results of the lateral shear measurements of f_0 are shown in Figs. 8 and 9 for wall temperatures of 100°C and 50°C and for CO_2 and N_2 gases. At most only the second calculation of f_0 was necessary. The curves are theoretical and the points experimental. The theoretical curves are from Marcuse [3].

In general, the agreement is good and indicates that the theory for f_0 is valid. There seems to be a greater discrepancy at the lower θ_0, however, where the assumptions used in the theory should be most accurate. It is possible this is an experimental error which becomes large in measuring larger focal distances. At long focal distances any focusing action in the optical components used in the interferometer or errors in collimating the input beam would become more important. Nothing of this type could be found, however, and the discrepancy remains unexplained.

2) *Mach-Zehnder Interferometer Measurements of the Aberrations:* As we pointed out earlier, the Mach-Zehnder interferometer was found more accurate and more convenient for finding α and β. A Mach-Zehnder interferometer is shown in Fig. 10. In Fig. 11 are shown some typical ring patterns. The pattern for CO_2 at 0.75 liter per minute gas flow shows the effect of gravity. Gravity causes a crowding of interference rings at the pattern bottom. The pattern for CO_2 at 4.0 liters per minute gas flow shows the gravity effect to be greatly reduced at high flow rates. The symmetric aberration β is evident here. This causes the center spot to be large and the outer rings to be smaller and crowded together. The pattern for N_2 at 1.5 liters per minute shows that the gravity effect is much less for N_2. At 6 liters per minute the symmetric aberration can be seen in the N_2 pattern.

a) *Evaluation of β:* The values of β were computed from the results derived in Appendix A. The β parameter was evaluated from measurements of ring spacing in the horizontal plane. If b_1 and b_2 are the horizontal distances from the pattern center to two rings separated by n rings, then

$$\beta \approx \frac{-1 + \left[1 + \dfrac{4[2n\lambda R_0 - (b_1^2 - b_2^2)]}{b_1^2 - b_2^2}\right]^{1/2}}{2\bar{b}^2}\frac{R_0^3}{f_0^3}$$

where

$\bar{b} = (b_1 + b_2)/2$
$\lambda = .633 \times 10^{-3}$ mm
$R_0 = f_0 - D$
D = distance from the end of the lens to the plane of measurement.

The results for β are shown in Fig. 12. The points are experimental and the dashed curve is the smooth curve which seems to best fit the data. It can be seen that β is positive for high flows, negative for low flows and, hence, there is some flow rate which gives a lens with no symmetrical aberration.

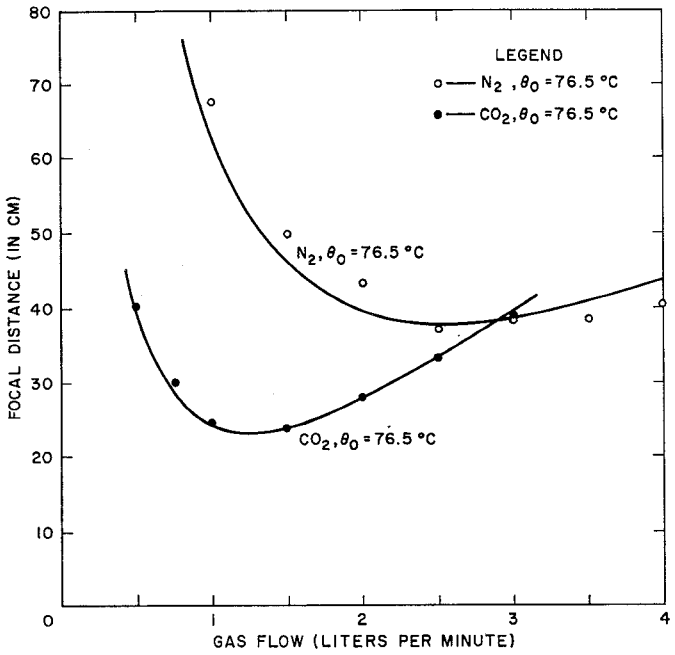

Fig. 8. Paraxial focal distance vs. gas flow rate. $T_w = 100°C$. Solid curves are theoretical.

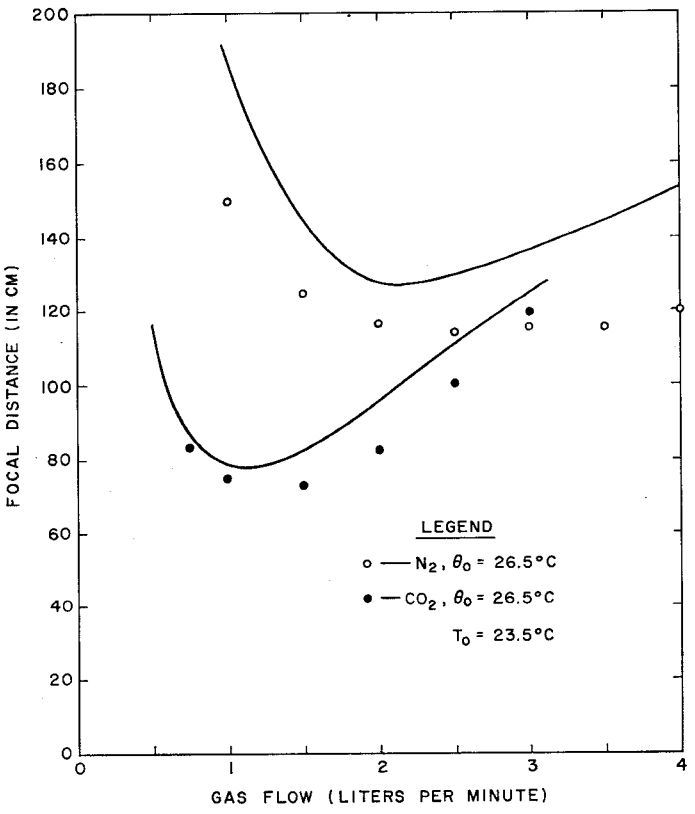

Fig. 9. Paraxial focal distance vs. gas flow rate. $T_w = 50°C$. Solid curves are theoretical.

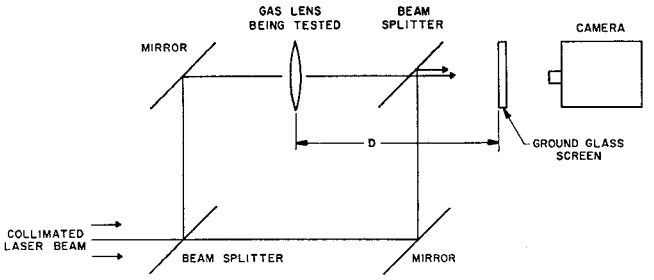

Fig. 10. Mach-Zehnder interferometer.

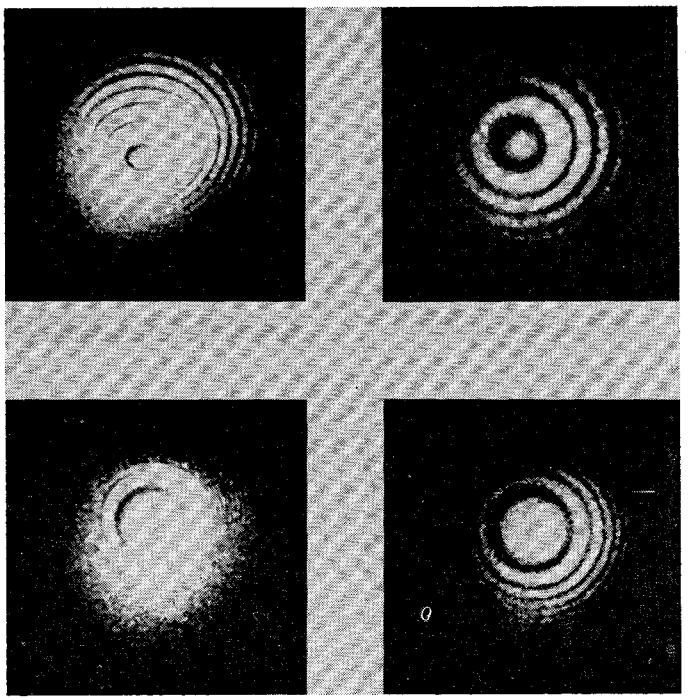

Fig. 11. Typical Mach-Zehnder interferograms.

$CO_2 - \theta_0 = 76.5°C$	$N_2 - \theta_0 = 76.5°C$
0.75 Liters per minute	1.5 Liters per minute
4 Liters per minute	6 Liters per minute

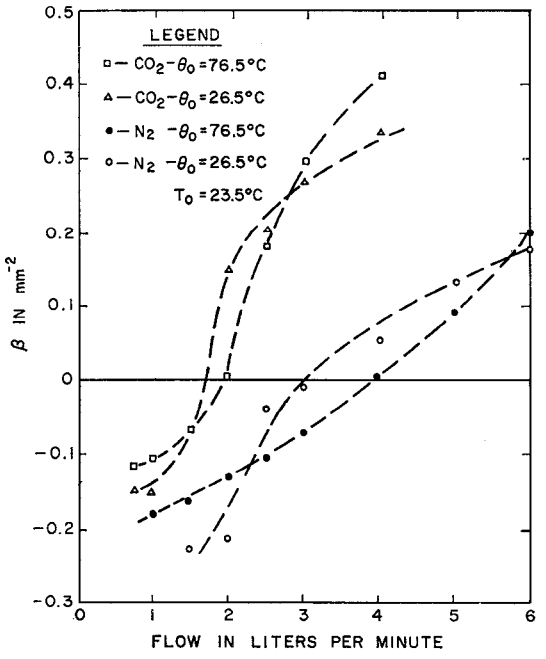

Fig. 12. Symmetric aberration parameter vs. gas flow rate.

From the theory of Marcuse [3], the theoretical values of β can be calculated. The experimental curves have the same general shape as the theoretical, but are displaced to higher flow values by approximately 25 percent.

b) *Evaluation of* α: The gravity aberration parameter α can be evaluated from vertical measurements of the ring patterns. It is shown in Appendix A that if c_1 is the vertical distance from the pattern center to the top of an interference ring, and c_2 is the vertical distance from the pattern center to the bottom of the same ring, then

$$\alpha \approx \frac{3}{2}\frac{(c_1 - c_2)}{\bar{c}^2}\left[1 - \frac{1}{5}\beta\frac{f_0^3}{R_0^3}\bar{c}^2\right]\frac{R_0^2}{f_0^2}$$

where

$\bar{c} = (c_1 + c_2)/2$
$R_0 = f_0 - D$
D = distance from the end of the tube to the plane of measurement.

The values of f_0 and β were taken from the previous measurements. The results for α are shown in Fig. 13. The points are experimental and the dashed curves represent an attempt to fit smooth curves to the data. The values of α observed for N_2, $\theta_0 = 26.5°C$ were all too small for the measurements to be meaningful.

There is no theory for the gravity aberrations to compare to the observations. We can correlate to some extent, however, the temperature profile measurements of Section II with these results. The variation of α with gas flow rate agrees with the variation of σ/a shown in Fig. 4. The gravity aberration falls off at low flows because after a short distance down the tube the gas on axis is very near the wall temperature. The α again decreases at high flow rates since the gas spends little time in the tube.

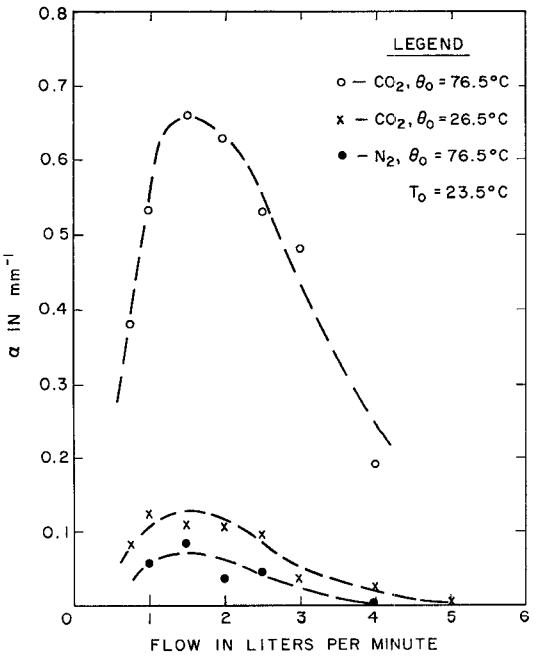

Fig. 13. Gravity aberration parameter vs. gas flow rate.

3) *Other Observations from the Ring Patterns:* From the ring interference pattern for CO_2 at $\theta_0 = 76.5°C$ shown in Fig. 11, it can be seen that when the gravity aberration is high there is also some astigmatism in the lens near the axis. This implies that the focal length on axis is different in the horizontal and vertical planes. This causes the center rings of the pattern to be oval shaped. No attempt was made to evaluate this aberration since it only occurred when the gravity aberration was very large. The focal distance measurements shown in Figs. 8 and 9 are measured in the horizontal plane.

Because the gas lens involves a flowing gas, there has been some question as to its stability in time. The Mach-Zehnder interferometer patterns were as stable in time with the lens in one arm as with no lens in the interferometer. This means the lens is at least as stable in time as the interferometer.

IV. Evaluation of Δ

As pointed out earlier gravity causes the center of the lens to occur below the center of the tube. This distance is labeled Δ and was measured as follows:

1) A photograph of the focused spot was made in the plane where the spot is minimum size.
2) A 0.250-inch diameter brass insert with a 0.010-inch diameter hole on axis was then inserted in the end of the heated tube and the gas turned off.
3) On the same film and in the same plane as 1) a photograph of the diffraction rings from the 0.010-inch diameter hole was taken.

The center of the focused spot locates the center of the lens and the center of the diffraction rings locates the center of the tube. The distance between them is Δ.

Care must be taken to assure that the light goes down the center of the tube. This was done by double exposing a picture of the unfocused laser spot (gas lens off) and the diffraction rings from the 0.010-inch hole. The position of the tube was then adjusted until the diffraction pattern fell in the center of the unfocused spot.

The results for CO_2 at $T_w = 100°C$ are shown in Fig. 14. For lower T_w and N_2 the effect could not be measured. This is because Δ is smaller and the center diffraction spot was larger, since the focal plane (where the photograph is made) is further from the 0.010-inch hole.

From Fig. 4 it can be seen that when Δ is large, it is very nearly equal to the δ at the end of the hot tube. That is, the center of the lens very nearly corresponds to the minimum temperature position at the end of the hot tube.

As expected from this measurement, the lens tends to give the least distortion when the light is centered below the tube center. If a Gaussian spot is sent into the lens, the spot, after going through focus, has what appears to be the most uniform intensity distribution if the light goes through the tube below center.

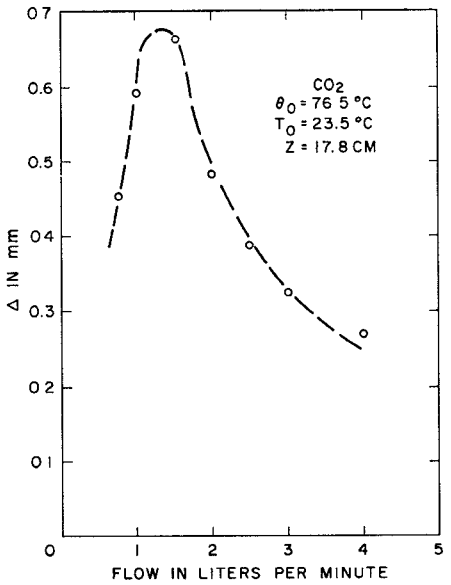

Fig. 14. Distance the lens center is below the tube center vs. the gas flow rate.

V. Summary

Blowing a cool gas through a hot tube makes a surprisingly strong optical lens. For moderate flow rates, moderate temperatures and lengths, and common gases, a lens with a focal distance of 50 cm or less, with small aberrations, is possible. Focal distances as low as 24 cm have been observed.

The lens has a variation of focal distance with radius which is symmetric about the center. This aberration can typically result in a 10–20 percent variation in focal distance over the center 1-mm radius portion of the lens. At a gas flow rate giving nearly the minimum focal distance for the wall temperature, tube length, and gas used this symmetric aberration can be near zero.

The lens laid horizontal also has a vertical asymmetric variation in focal distance with radius which is caused by gravity. In severe cases this can result in a 70 percent variation over the center 1-mm radius portion of the tube. More typically this will result in an 8–10 percent variation. This effect is maximum near the minimum focal distance flow rate.

Although the aberrations of the gas lens would make its use for image formation doubtful, these aberrations may not be harmful in an optical transmission line. The requirements for a useful optical power transmission medium are not the same as those for image reproduction. The deleterious effects of lens aberrations on images do not necessarily imply serious losses in a power transmission system.

These lenses appear to be well suited for long distance optical transmission. The focal lengths are short enough to give a reasonable minimum bending radius for the guide to allow the pipe to follow the terrain. The lenses have no surfaces for scattering and reflection of the beam.

As an example, a lens with a 50-cm focal length with small convection aberrations is possible using nitrogen. A series of these 0.250-inch diameter lenses spaced at 50 cm would give an optical transmission line with the following properties at 6328Å:

Beam spot radius, 0.33 mm
Minimum bending radius [6] of the lens for 0.33-mm beam deflection = 1500 meters.

Since the diffraction losses of such a line would be extremely small, the losses will primarily be determined by the scattering from the gas, imperfections in the lenses, and misalignment of the lenses. It would seem that these losses could be kept low.

The general conclusion, which can be drawn from these measurements, is that the theory derived for the gas lens is valid except for the gravity effect, not included in the theory. The temperature distribution of the gas as it moves through the tube is very nearly as predicted. The paraxial focal distance is also very close to the theory.

The theory and observations of the symmetric aberration show a general agreement. The variations with gas, wall temperature, and flow rate are as predicted and the zero crossings are in the predicted order. The quantitative agreement, however, is not so good. This may be error in experiment since the measurement of β involves small differences in large numbers. The parameter β could perhaps be measured more accurately by a technique which would remove the first-order curvature of the phase front and leave only the variation in curvature. Similarly, it is possible for the theory to be in greater error in predicting aberrations than in predicting the paraxial focal distance of the lens. Because differences of large numbers are involved the assumptions used in the theory are less accurate.

There is no theory for the gravity effect with which a comparison can be made. There is good correlation between the gravity asymmetry observed in the temperature measurements and the gravity asymmetry observed in the optical measurements.

Appendix A

A. Calculation of Aberrations from Mach-Zehnder Interference Patterns

1) *Equation of the Phase Front:* Consider a lens whose focal length in a cross-section is given by

$$f = f_0(1 + \alpha x' - \beta x'^2) \tag{1}$$

where
x' = distance from the center of the lens
f_0 = focal length at $x' = 0$.

Assume a plane wave incident on the lens as shown in Fig. 15 and consider only two dimensions. At a distance $D < f$ from the lens it can be seen from Fig. 16 that the

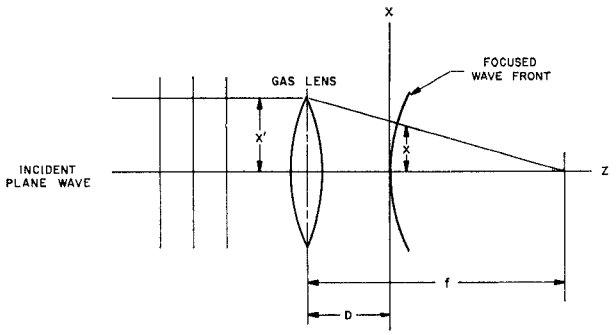

Fig. 15.

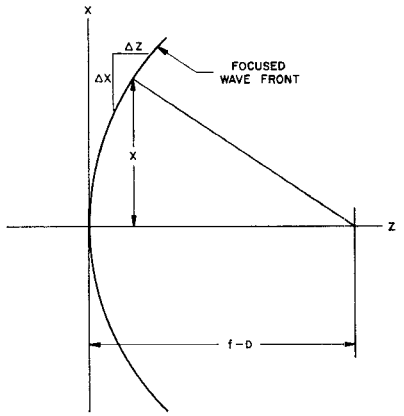

Fig. 16.

equation of the phase front can be found from

$$\frac{dz}{dx} = \frac{x}{f - D}$$

if $z/(f - D) \ll 1$. It is approximately true that $x' = f_0/(f_0 - D)x$ and hence

$$\frac{dz}{dx} = \frac{x}{R_0\left[1 + \alpha\frac{f_0^2}{R_0^2}x - \beta\frac{f_0^3}{R_0^3}x^2\right]} \tag{2}$$

where

$$R_0 = f_0 - D.$$

2) *Evaluation of* β

Consider a horizontal cross section where the convection effect and hence α is negligible. Then (2) becomes

$$\frac{dz}{dx} = \frac{x}{R_0\left[1 - \beta\frac{f_0^3}{R_0^3}x^2\right]}.$$

Integrating:

$$z = -\frac{R_0^2}{2\beta f_0^3}\log\left[1 - \beta\frac{f_0^3}{R_0^3}x^2\right]$$

$$z \approx \frac{x^2}{2R_0}\left[1 + \frac{\beta f_0^3}{R_0^3}\frac{x^2}{2} + \left(\frac{\beta f_0^3}{R_0^3}\right)^2\frac{x^4}{3}\right].$$

If a reference plane wave is mixed with this, it will produce interference rings. Let the radii of two such rings, separated by n rings be, respectively, b_1 and b_2. Then

$$n\lambda = \frac{b_1^2}{2R_0}\left[1 + \frac{\beta f_0^3}{R_0^3}\frac{b_1^2}{2} + \left(\frac{\beta f_0^3}{R_0^3}\right)^2\frac{b_1^4}{3}\right] - \frac{b_2^2}{2R_0}\left[1 + \beta\frac{f_0^3}{R_0^3}\frac{b_2^2}{2} + \left(\beta\frac{f_0^3}{R_0^3}\right)^2\frac{b_2^4}{3}\right]$$

or

$$\left(\beta\frac{f_0^3}{R_0^3}\right)^2\frac{b_1^6 - b_2^6}{3} + \frac{\beta f_0^3}{R_0^3}\frac{b_1^4 - b_2^4}{2} - [2n\lambda R_0 - (b_1^2 - b_2^2)] = 0,$$

and hence,

$$\beta \approx \frac{-1 + \left[1 + \frac{4[2n\lambda R_0 - (b_1^2 - b_2^2)]}{b_1^2 - b_2^2}\right]^{1/2}}{2\bar{b}^2}\frac{R_0^3}{f_0^3},$$

if

$$\left(\frac{b_1 - b_2}{\bar{b}}\right) < 1$$

where

$$\bar{b} = \frac{b_1 + b_2}{2}.$$

3) *Evaluation of* α

Consider a vertical cross section of the wavefront described by 2. If terms only to first order are retained in α and β then

$$\frac{dz}{dx} \approx \frac{x}{R_0}\left[1 - \alpha\frac{f_0^2}{R_0^2}x + \beta\frac{f_0^3}{R_0^3}x^2 - 2\alpha\frac{f_0^2}{R_0^2}\beta\frac{f_0^3}{R_0^3}x^3\right].$$

Integrating:

$$2R_0z = x^2 - \frac{2}{3}\alpha\frac{f_0^2}{R_0^2}x^3 + \beta\frac{f_0^3}{R_0^3}\frac{x^4}{2} - \frac{4}{5}\alpha\frac{f_0^2}{R_0^2}\beta\frac{f_0^3}{R_0^3}x^5.$$

If this phase front is mixed with a reference plane wave, interference rings are formed. Let c_1 be the distance from the pattern center to the top of some interference ring, and let c_2 be the distance from the pattern center to the bottom of the same ring. Then:

$$c_1^2 - \frac{2}{3}\alpha\frac{f_0^2}{R_0^2}c_1^3 + \beta\frac{f_0^3}{R_0^3}\frac{c_1^4}{2} - \frac{4}{5}\alpha\frac{f_0^2}{R_0^2}\beta\frac{f_0^3}{R_0^3}c_1^5 = c_2^2 + \frac{2}{3}\alpha\frac{f_0^2}{R_0^2}c_2^3 + \beta\frac{f_0^3}{R_0^3}\frac{c_2^4}{2} + \frac{4}{5}\alpha\frac{f_0^2}{R_0^2}\beta\frac{f_0^3}{R_0^3}c_2^5$$

which gives

$$\alpha = \frac{c_1^2 - c_2^2 + \beta\frac{f_0^3}{R_0^3}\frac{c_1^4 - c_2^4}{2}}{\frac{2}{3}(c_1^3 + c_2^3) + \frac{4}{5}\beta\frac{f_0^3}{R_0^3}(c_1^5 + c_2^5)}\frac{R_0^2}{f_0^2}$$

or

$$\alpha \approx \frac{3}{2} \frac{(c_1 - c_2)}{\bar{c}^2} \left[1 - \frac{1}{5} \beta \frac{f_0^3}{R_0^3} \bar{c}^2\right] \frac{R_0^2}{f_0^2}$$

if

$$\frac{c_1 - c_2}{\bar{c}} < 1.$$

Where

$$\bar{c} = \frac{c_1 + c_2}{2}.$$

Appendix B

A. Evaluation of f_0 from Shear Interferometer Patterns

Consider a plane wave which has gone through the lens with aberrations and has traveled a distance $D > f$ beyond the lens. The equation of the phase front in the horizontal plane, where there is no gravity effect, can be found in the same way as (2). In two dimensions this becomes

$$\frac{dz}{dx} = \frac{x}{R_0\left(1 + \beta \frac{f_0^3}{R_0^3} x^2\right)} \tag{3}$$

where now $R_0 = D - f_0$.

Let this wavefront be laterally sheared in the horizontal plane a distance s as shown in Fig. 17. The spacing of the fringes δx in the region where the fronts overlap is given by

$$\delta x \left[\left(\frac{dz}{dx}\right)_{\text{primary wave}} - \left(\frac{dz}{dx}\right)_{\text{sheared wave}}\right] = \lambda.$$

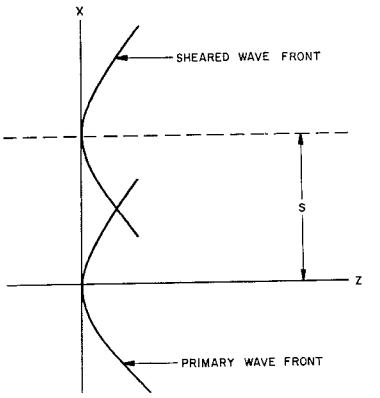

Fig. 17.

The spacing of the fringes in the center δx_0 where $x = s/2$ is therefore

$$\frac{\delta x_0 s}{\lambda} = R_0\left[1 + \beta \frac{f_0^3}{R_0^3} \frac{s^2}{4}\right]$$

and

$$f_0 = D - R_0 \approx D - \frac{\delta x_0 s}{\lambda}\left[1 - \beta \frac{f_0^3}{R_0^3} \frac{s^2}{4}\right].$$

References

[1] D. W. Berreman, "A lens or light guide using convectively distorted thermal gradients in gases," *Bell Sys. Tech. J.*, vol 43, pp 1469–1475, July 1964.
[2] D. Marcuse and S. E. Miller, "Analysis of a tubular gas lens," *Bell Sys. Tech. J.*, vol. 43, pp. 1759–1782, July 1964.
[3] D. Marcuse, "Theory of a Thermal-Gradient Gas Lens," *IEEE Trans. on Microwave Theory and Techniques*, this issue, page 734.
[4] A. C. Beck, "Thermal gas lens measurements," *Bell Sys. Tech. J.*, vol. 43, pp. 1818–1820, July 1964.
[5] M. Jacob, *Heat Transfer*, vol I, New York: Wiley, 1949, pp. 451–464.
[6] D. Marcuse, "Propagation of light rays through a lens—waveguide with curved axis," *Bell Sys. Tech. J.*, vol 43, pp. 741–754, March 1964.